Ann. Geophys., 31, 1721–1730, 2013
www.ann-geophys.net/31/1721/2013/
doi:10.5194/angeo-31-1721-2013
© Author(s) 2013. CC Attribution 3.0 License.

Annales Geophysicae
Open Access

Comparative time-series analysis of MeV electron data by Ulysses and Pioneer 10/11 in the Jovian magnetosphere

P. Dunzlaff[1,2], **B. Heber**[2], **A. Kopp**[2,1], **and M. S. Potgieter**[1]

[1]Centre for Space Research, North-West University, Potchefstroom, South Africa
[2]Institut für Experimentelle und Angewandte Physik, Christian-Albrechts-Universität zu Kiel, Kiel, Germany

Correspondence to: P. Dunzlaff (dunzlaff@physik.uni-kiel.de)

Received: 17 May 2013 – Revised: 15 August 2013 – Accepted: 3 September 2013 – Published: 16 October 2013

Abstract. The dynamics of the Jovian magnetosphere is dominated by the planet's fast rotation with a period of ~ 10 h. Within the magnetosphere, this periodicity can in particular be seen in the temporal variation of the spectral index of MeV electrons: every ~ 10 h the counting rates show a maximum (minimum), while the spectral index shows a minimum (maximum) known as the Jovian "clock" mechanism. In this study we re-analyse Ulysses and Pioneer 10/11 data and show that another periodic modulation in the MeV electrons can be identified, manifested by local maxima of the spectral index and local minima of the counting rates. For Ulysses, this modulation can be observed throughout the magnetosphere near the magnetic equator, suggesting an azimuthal asymmetric distribution of MeV electrons near the current sheet. This modulation is found to trail the "clock" mechanism by ~ 3.25 h. The Pioneer 10 data, however, only show occasional evidence of the presence of these local maxima while there is no evidence of this modulation in the Pioneer 11 data. A comparison of the times of observed minor peaks and Ulysses' distance from the current sheet using a simple rigid disc model as well as the model of Khurana and Schwarzl (2005) is performed.

Keywords. Interplanetary physics (cosmic rays) – magnetospheric physics (planetary magnetospheres)

1 Introduction

The dynamics of the Jovian magnetosphere is dominated by the planet's fast rotation with a period of ~ 10 h and the influence of the moon Io as a strong source of plasma. The majority of this plasma is confined to the Jovian current (or plasma) sheet located close to the dipole magnetic equator with a thickness of 4–6 Jovian radii ($1\ R_J = 71\,492$ km) depending on the local time (Khurana and Schwarzl, 2005; Waldrop et al., 2005).

Within the magnetosphere, this periodicity can in particular be seen in the temporal variation of the spectral index of MeV electrons. Based on the Pioneer spacecraft flybys in the 1970s, several models were developed to explain this phenomenon.

The "disc model", proposed by van Allen et al. (1974), connects the observed modulation to the actual position of the spacecraft with respect to the magnetic latitude, in particular the proximity to the current sheet. This model, however, came into trouble when Pioneer 11 explored the Jovian magnetosphere at relatively high magnetic latitudes and still observed high particle fluxes. Combining Pioneer 10 and 11 magnetic field data, Dessler and Hill (1975) argued that a longitudinal asymmetry of the magnetic field strength near the surface of the planet results in the 10 h periodicity of energetic charged particles due to the indirect influence of higher order magnetic multipoles (see also Hess et al. (2011) for a recent study of the Jovian magnetic field topology). This so-called magnetic anomaly (or active sector) causes an azimuthal asymmetry of the charged particle population in the outer regions of the magnetosphere co-rotating with the planet (Vasyliunas and Dessler, 1981). The most prominent, however, is the so-called "Jovian clock" model predicting that this periodicity is caused only by temporal variations in the Jovian magnetosphere. Chenette et al. (1974) reported that the periodic variations of the spectral index inside and outside (during so-called Jovian electron bursts) the Jovian magnetosphere are in phase. However, Simpson et al.

(1992b) reported phase shifts of some hours in Jovian electron bursts observed close to the planet with respect to the phase of the spectral rocking inside the magnetosphere.

In order to search for additional patterns besides the well-known "clock" periodicity in the spectral index (approximated by the ratio of two energy channels) and counting rates, we re-investigated data obtained by the Kiel Electron Telescope (KET) and High Energy Telescope (HET) instruments aboard Ulysses during the spacecraft's Jupiter flyby in February 1992 and compare the results with Pioneer 10 & 11 data during their flybys in late 1973 and 1974, respectively. Besides the "clock" modulation, we found a second periodic variation being manifested by (a) a local minimum of the counting rates associated with (b) concurrent local maxima in the spectral index and (c) an occurrence of these events at subsolar System III longitudes of 40–100° and low magnetic latitudes.

2 Instrumentation and methods

In this work we make use of Ulysses and Pioneer 10 & 11 charged particle and magnetic field data. For the case of Ulysses, we analysed data of the Kiel Electron Telescope (KET) as well as the High Energy Telescope (HET) described in detail by Simpson et al. (1992a). The KET is designed to measure electrons and protons as well as α particles in an energy range from a few MeV/nuc up to a few GeV/nuc. For our analysis we made use of 10 min averages of the E4 and E12 channels, measuring electrons in the energy ranges 2.5–7 MeV and 7–500 MeV, respectively. For the HET data we also made use of 10 min averages of the H3 and H5 channels. The H3 and H5 channels had also been used in the study of Simpson et al. (1992b) and measure protons in the energy range 24–31 MeV and 68–92 MeV, respectively, under interplanetary conditions. However, these channels are also sensitive to electrons in the range of 3–5 MeV and 10–16 MeV. It is expected that these channels predominantly counted electrons while the spacecraft was in the Jovian magnetosphere (Simpson et al., 1992b). For both instruments we used a time resolution of 10 min.

For the magnetic field measurements, we made use of the VHM/FGM instrument aboard Ulysses (Balogh et al., 1992).

For the analysis of the Pioneer spacecraft data, we used data of the almost identical University of Chicago Instruments (CPIs) aboard the two Pioneers as well as magnetometer data of the MAG experiment. The CPI electron channels we used in this work are the id4 and id5 channels. The id4 channel counts electrons in a range of energy from 2 to 7 MeV (and protons and heavier ions of several tens of MeV), while the id5 channel counts electrons between 6 and 28 MeV, along with protons and heavier ions of energies above those counted by id4. For the Pioneer data we used a time resolution of 15 min. A brief discussion of the CPI can be found in Lentz et al. (1973).

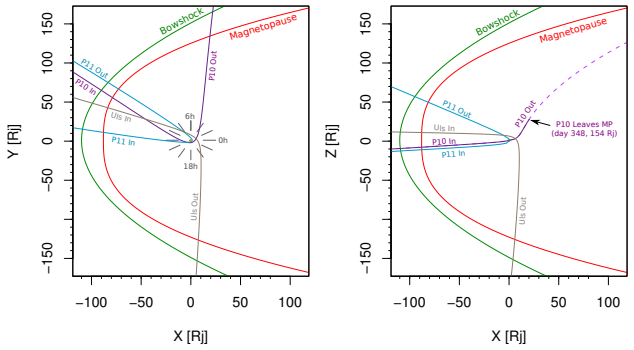

Fig. 1. Trajectories of Ulysses and Pioneer 10/11 during their Jupiter encounters. The coordinate system is given in Jovian radii (1 $R_J = 71\,492$ km). For illustration, the bowshock and the magnetopause are indicated for an assumed sunward extension of 110 R_J and 88 R_J, respectively. The shapes of the bowshock and magnetopause are calculated with the equations given by Joy et al. (2002). The left panel shows an equatorial view of the trajectories, the right one the meridional view.

Figure 1 shows the trajectories of Ulysses and Pioneer 10 & 11 for the times of their Jupiter flybys in a coordinate system in which the x axis is the Sun–Jupiter line pointing away from the Sun (given in Jovian radii). The z axis is directed northwards, perpendicular to the orbital plane of the planet, and the y axis completes a right-handed system. As can be seen, the three spacecraft entered the magnetosphere in the post-dawn sector at low latitudes. Their outbound trajectories, however, were quite different from each other. While Pioneer 10 was deflected towards the dawn side at moderate latitudes, the trajectory of Pioneer 11 is characterised by a high-latitude path along the post-dawn sector towards Saturn.

3 Ulysses observations

Figure 2 shows an overview of magnetic field and KET/HET data measured by Ulysses between day 34 and 36.5 in 1992 (i.e. just after the transition of the spacecraft from the interplanetary medium into the magnetosphere until the temporary switch-off of the KET). This time interval covers the region of the magnetosphere generally called the outer magnetosphere. According to the magnetic field data, no clear structure is evident, indicating a highly disturbed orientation of the field in the outer magnetosphere. An investigation of the E4 / E12 and H3 / H5 ratios, however, reveals a consistent pattern of recurrent variations of the energy spectrum with a periodicity of 10 h as indicated by the dashed vertical lines being aligned with the maxima of the ratio. The markers are 9 h 55 min apart from each other. Comparing the temporal evolution of the ratios with the corresponding counting rates of the HET instrument, it becomes evident that both quantities are anti-correlated: the counting rates tend to increase

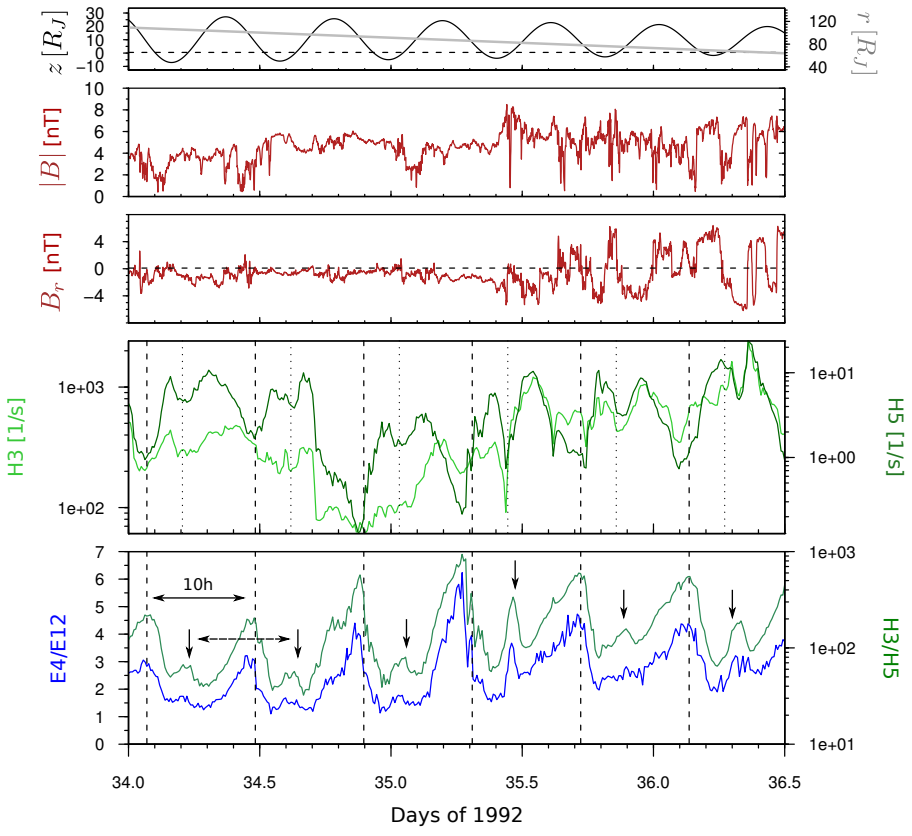

Fig. 2. Ulysses data for the spacecraft's inbound path from day 34 to 36.5. The bottom panel shows the KET E4 / E12 and HET H3 / H5 ratios as a proxy to the spectral index of MeV electrons followed by the H3 and H5 counting rates. The next two panels show the radial component of the magnetic field as well as the magnetic field magnitude. The top panel shows the distance of the spacecraft from the magnetic equator (rigid disc, black) and from the planet (grey) in Jovian radii. Besides the well-known clock-like modulation ("major peaks", indicated by the dashed lines), a second periodicity of ~ 10 h associated with low magnetic latitudes is apparent and indicated by the vertical arrows ("minor peaks").

when the spectral index decreases and vice versa. This finding had already been discussed in earlier publications (e.g. by Simpson et al., 1992b) and is generally attributed to the Jovian clock mechanism.

However, besides the large peaks, denoted as "major peaks" in the following, peaks of much smaller amplitudes can be identified in the time series and are indicated by the black arrows in the bottom panel. An interesting feature of these "minor" peaks is the fact that they occur when the flux level is generally high, but during local minima (i.e. during short-term decreases of the electron counts). These local minima are indicated by the dotted vertical lines in the panel showing the H3 and H5 counting rates. This behaviour strongly resembles the major peaks. The dotted lines in the panel showing the HET counting rates are positively shifted by about 3.25 h with respect to the dashed lines and indicate the local counting rate minima. This shift will be further quantified later using a correlation analysis. Nevertheless, it can be noted that the phase difference between the major and minor peaks is not a symmetric behaviour since this would imply a phase shift of ~ 5 h. Comparing the occurrence of the minor peaks with the distance from the nominal current sheet (top panel), one observes that they generally occur when the spacecraft is located close to the current sheet (i.e. at low magnetospheric latitudes). These minor peaks were previously only mentioned as a side note in Anagnostopoulos et al. (1998) when investigating the temporal behaviour of ions close to Jupiter without taking into account magnetic field measurements.

Subsequently, Fig. 3 covers the time interval from days 36–38.5 and shows the same quantities as Fig. 2. During this time, the spacecraft was mainly located in the middle magnetosphere, and the presence of the Jovian current sheet can clearly be seen by the four current sheet crossings indicated by the red solid lines (i.e. two crossing per rotation, dates taken from Krupp et al., 1993). These two pairs of crossings from the Northern Hemisphere to the south and back are roughly 10 h apart. While these events indicate full current sheet crossings as can be seen by the inversions of the direction of the radial component B_R of the magnetic field,

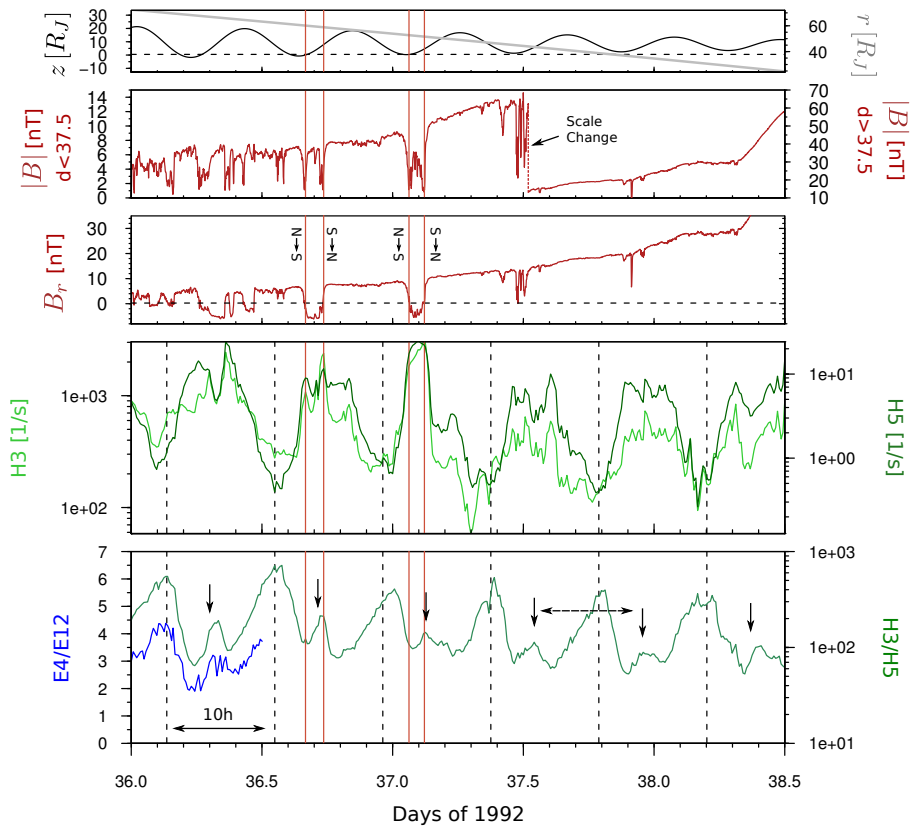

Fig. 3. Same as Fig. 2 but for the time interval day 36 to 38.5. The major and minor peaks are still present. Four current sheet crossings are indicated by the red vertical lines and reveal that the minor peaks occur when the spacecraft moves across the current sheet from south to north. Note the scale change in $|B|$ at day 37.5.

at least three current sheet approaches can be observed as the spacecraft approaches the planet (e.g. around day 37.5). These events are characterised by decreases in the magnetic field magnitude and radial component, although the polarity does not change (cf. Hoogeveen et al., 1996). The charged particle data plotted in Fig. 3 are again the HET counting rates and the HET and KET ratios of two energy channels. Note that due to the prevention of possible damages the photomultipliers of the KET were switched off on day 36.5. The dashed lines and the arrows indicating the major and minor peaks respectively are in phase with the markings of Fig. 3.

Focusing on the two current sheet crossings around day 36.7, the counting rates of the H3 and H5 channels show a double-peaked profile correlated with the lowest magnetic field strength. Comparing the minor peaks of the spectral index and the magnetic field data during the two pairs of current sheet crossings, an interesting observation is the fact that the peaks in the spectral index are in very good coincidence with the spacecraft's crossing from the Southern Hemisphere towards the Northern Hemisphere. This suggest that the minor peaks are a spatial effect: on the one hand, the correlation with the current sheet implies that these events are confined to the magnetic equator. On the other hand, an intrinsic longitudinal asymmetry of the electron distribution must be present, since it is unreasonable to assume that the spacecraft should measure different charged particle properties depending on the sense of motion across the current sheet, given that the particles are almost equally distributed around the sheet. Before further properties of the minor peaks are discussed, we will quantify our results using a correlation analysis. The result of a linear (Pearson's) autocorrelation of HET's H5 and H3 channels is shown in Fig. 4 for the time period of days 34–36 (i.e. during the spacecraft's paths through the outer magnetosphere). The abscissa shows the time lag in hours and the ordinate the corresponding autocorrelation coefficient. It can be seen that the 10 h variation of the counting rates can be recovered in this analysis of H5, as indicated by the recurrent peaks of positive or negative correlation coefficients every 10 h, marked by the solid and dashed vertical lines, respectively. However, further peaks can be identified between those related to the prominent 10 h variation, tagged by the dotted vertical lines. These peaks occur ~ 3.25 h before and after the larger 10 h peaks. This time difference corresponds to the time interval between the double peaks of the principal flux enhancements, giving further evidence that this is a systematic effect. The analysis of H3, however, shows no

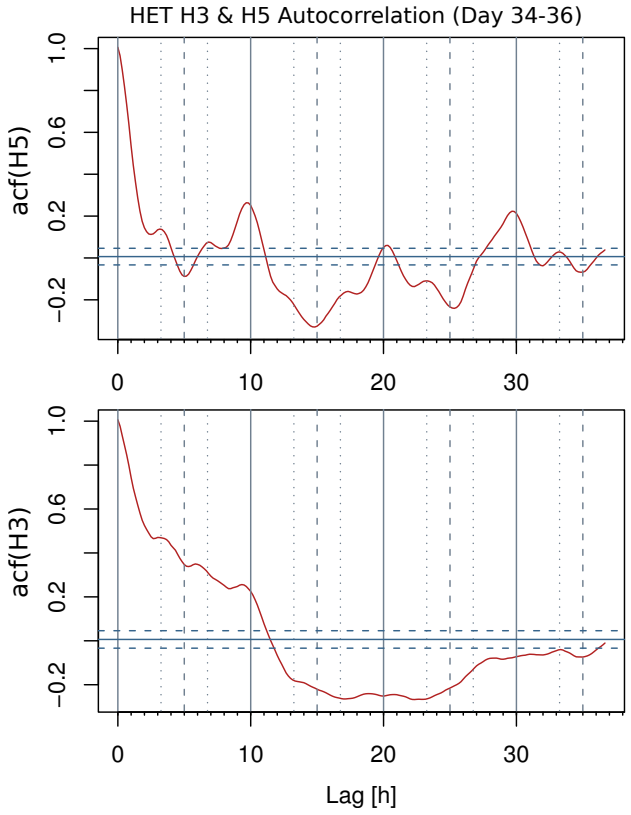

Fig. 4. Autocorrelation of the HET H5 (top) and H3 (bottom) channels. The solid lines indicate the 10 h periodicity that is well pronounced for the H5 channel. The dashed lines lie in the middle of the 10 h intervals. However, another temporal variation can be identified in the H5 data as indicated by the dotted lines. These peaks are shifted by ± 3.25 h with respect to the major 10 h peaks. The same analysis for the H3 channel shows no clear modulation, suggesting that the spectral rocking is mainly due to the higher energy channel (i.e. H5).

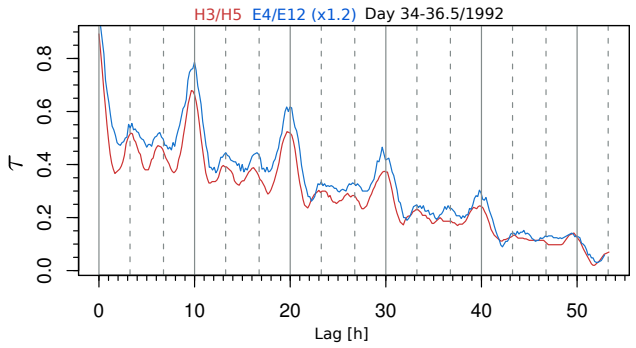

Fig. 5. Result of the ordinal autocorrelation analysis of the H3 / H5 (red) and E4 / E12 (blue) ratios for days 34–36. Similar to Fig. 4, this figure not only reflects the temporal variation related to the clock mechanism, but also shows evidence of a second periodic modulation related to the minor peaks in the spectral index. The shift between both variations is ~ 3.25 h.

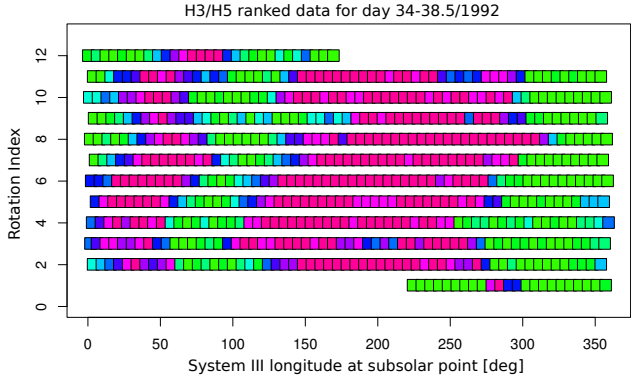

Fig. 6. Local rank structure of the HET H3 / H5 ratio from day 34 to 38.5. The time series starts at rotation 1 (bottom) and ends with rotation 12 (top). The colour code must be interpreted in a way that red squares indicate that the actual data point has a higher rank than its predecessor 10, while green indicates a lower rank (i.e. the local maxima of the H3 / H5 ratio occur when the colour switched from red to green). As expected, this is the case for longitudes of about 270°, reflecting the major peaks of the Jovian clock. Furthermore, the minor peaks are clearly present with local maxima at 40–100°.

clear modulation like H5. This suggests that the rocking of the H3 / H5 ratio is mainly related to periodic variations of H5 (i.e. the channel of higher energies, as well as a larger stationarity of the H5 channel). Indeed, a visual investigation of the H3 and H5 counting rates in Figs. 2 and 3 shows that the H5 channel tends to be better pronounced with respect to the amplitude of its temporal variations.

Considering the electron spectral index, the H3 / H5 and E4 / E12 ratios were analysed using an ordinal correlation method adopted from Bandt (2005). The benefit of an ordinal (i.e. non-parametric) correlation analysis is that the individual data points are not compared by their actual value but by their ranks (i.e. the relative magnitude with respect to the complete data set) (cf. chapter 14 in Press et al., 1992). The rank of a data point may be computed globally (i.e. by taking into account all available data). However, it is also possible to assign a local rank to a specific data point by comparing its value with a finite number of neighbouring data. For this study we used local ranks by comparing each data point with its 10 (Ulysses) or 8 (Pioneer) preceding data points. The result of an ordinal autocorrelation of the H3 / H6 and E4 / E12 ratios is shown in Fig. 5 for days 34 to 36. The 10 h rocking of the spectral index is clearly visible in both the HET and KET data. However, similar to the previously shown H5 counting rates, another periodicity is apparent. Again, these features occur about 3.25 h before or after the correlation maxima due to the clock mechanism, which we attribute to the minor peaks in the corresponding time series (Fig. 2). Note that the autocorrelation function in Fig. 5 is not normalised.

To provide another, more visual, impression of the temporal behaviour of the spectral index, Fig. 6 shows the local

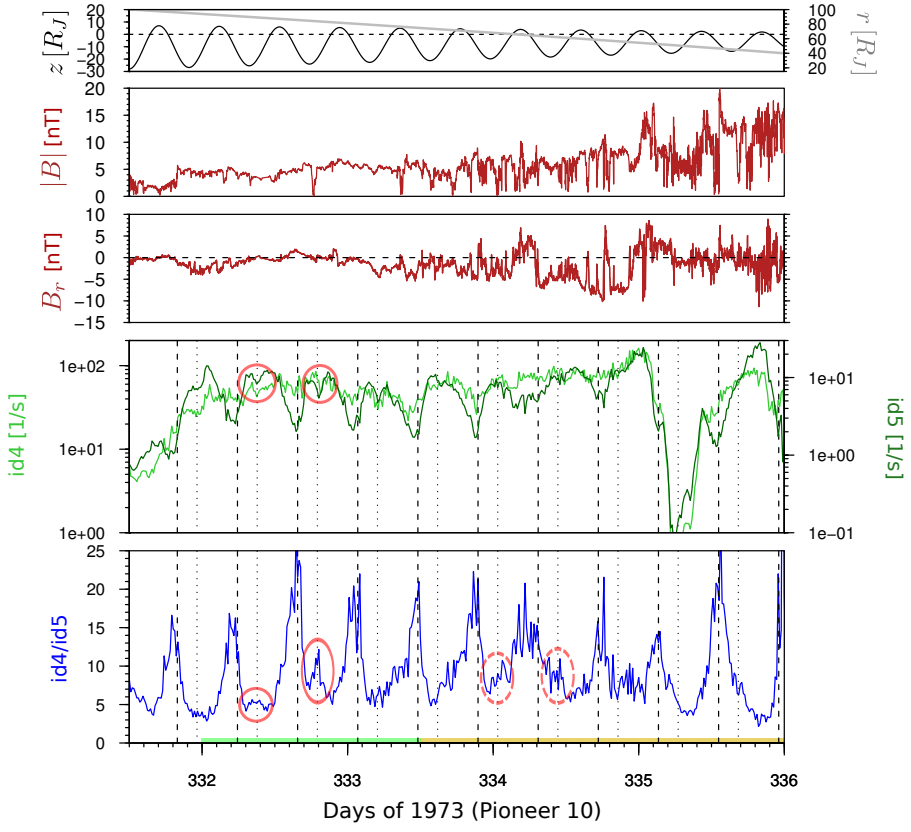

Fig. 7. Magnetic field and particle data of Pioneer 10 during the spacecraft's inbound trajectory similar to Figs. 2 and 3. Events that can be interpreted as minor peaks are indicated by red ellipses in the bottom panel. The ellipses in the panel showing the id4 and id5 counting rates indicate the corresponding local minima. The dashed ellipses in the time series showing the spectral index indicate questionable events with no clear counterparts (i.e. local minima) in the counting rates. Note, however, that most of the time local minima on top of the global count rate maxima can be identified. The green and yellow shades on the bottom of the figure indicate two time intervals analysed independently.

ranks of the individual data points of the H3 / H5 ratio as a function of the System III longitude in a colour-coded way. The abscissa is the System III longitude at the subsolar point of the Jovian magnetosphere; the ordinate indicates the number of rotations of the planet (starting with rotation #1 at day 34 and ending at day 38.5). In this representation, the use of local ranked values instead of using the absolute values of H3 / H5 has the advantage that subtly nuanced variations can be emphasised. To interpret this figure, note that the red squares indicate that the actual data point has a higher rank than its predecessor 10, while green indicates a lower rank (i.e. a decreasing of the H3 / H5 ratio). A lower rank (i.e. the local maxima of the H3 / H5 ratio) occurs when the colour switches from red to green. On the one hand, this figure clearly illustrates the well-known 10 h modulation (i.e. a maximum in the spectral index if the System III longitudes $\lambda_{III} = 240°–310°$ face the subsolar point). On the other hand, the presence of the minor peaks with a local maximum of the spectral index can be identified at System III longitudes $\lambda_{III} = 40°–100°$ in agreement with the respective time series.

4 Pioneer 10/11 observations

After having shown that a second periodic modulation in the spectral index (and counting rates) besides the clock phenomenon can be identified in the Ulysses data, suggesting a connection to the current sheet, the question arises of whether the Pioneer 10/11 data show the same kind of modulation.

Figure 7 shows Pioneer 10 measurements in a format similar to the previously shown Ulysses data. The shown time interval spans from day 331.5 to 336 in 1973 (i.e. from the entry into the magnetosphere up to a distance from the planet of about 40 R_J). At a first glance, the periodic rocking of the spectral index (i.e. the id4 / id5 ratio) is clearly visible and anti-correlated with the counting rates (Chenette et al., 1974). The dashed vertical lines are 9 h 55 min apart. A closer look, however, reveals the existence of local minima in the id5 counting rates on top of the global maxima. These minima are indicated by the dotted lines and are also 9 h 55 min apart from each other. The phase difference between the dashed and the dotted lines is 3.25 h, just as for Ulysses. Note, however, that these "valleys" are somewhat

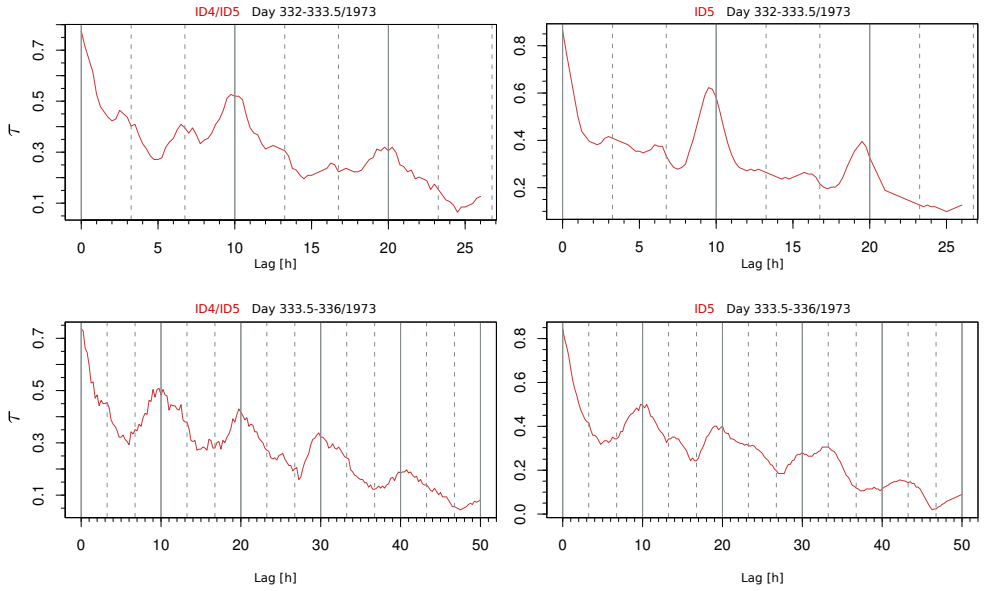

Fig. 8. Ranked autocorrelation analysis of Pioneer 10 data for days 332 to 333.5 (top) and 335.5–336 (bottom). The left panels show the id4 / id5 ratio data and the right the id5 counting rate data. The 10 h periodicity of the major peaks is present for all data sets. However, similar to the Ulysses data, a second modulation can be identified in the id4 / id5 and id5 data for days 332–332.5. This modulation is more weakly pronounced due to the short time period used for this analysis and the fact that the minor peaks are not as well established as for Ulysses. During the time interval from day 333.5 to 336, there is no satisfying evidence of minor peaks.

more weakly pronounced than the ones observed by Ulysses. Comparing the counting rates with the associated spectral index, consistent evidence of minor peaks is barely visible over the full time interval. However, some enhancements of the id4 / id5 ratio can be regarded as minor peaks. These events are indicated by the red ellipses in the id4 / id5 ratio and in the respective local counting rate minima. The dashed ellipses indicate questionable events that have no counterpart in terms of a local counting rate minimum.

Figure 8 shows the result of an autocorrelation of the Pioneer 10 data split into two time intervals according to the shaded areas in Fig. 7. The major 10 h peaks can be well identified. However, there is also some evidence of the existence of minor peaks shifted 3.25 h with respect to the majors in the first time interval. These peaks are much less pronounced than those found in the Ulysses data, regarding the visual impression of the corresponding time series. During the time interval from days 333.5 to 336, there is no satisfying evidence of minor peaks.

With respect to the focus of this work, it is interesting to note that Fillius and Knickerbocker (1979) already mentioned the occasional presence of "double-humped" peaks in the counting rates of Pioneer 10 electrons in the outer magnetosphere and already speculated on a possible influence of the current sheet at distance from the planet $> 63\ R_J$ when comparing the data of the University of San Diego instrument aboard Pioneer 10 & 11 with the disc, anomaly and clock model. These double-peak features are identical to the edges of what we call local minima and lead to the minor peaks in

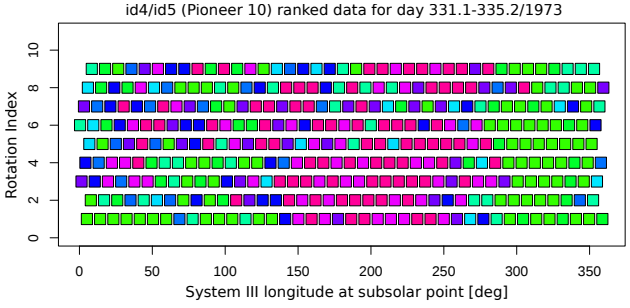

Fig. 9. Same analysis as shown in Fig. 6 but for the Pioneer 10 id4 / id5 data during the inbound pass. Again, a recurrent maximum of the id4 / id5 ratio is present at System III longitudes of $\sim 270°$. However, similar to the Ulysses data, a second periodic enhancement is visible at 40–100°. Compared to Ulysses, this modulation is much more weakly pronounced and less sustainable.

the spectral index of the electrons and show the features of the events discussed for Ulysses.

The Pioneer 11 inbound data (Fig. 10) cover the time period from day 335.5 to 336.5 in 1974. The id4 / id5 ratio plotted in the bottom panel shows the presence of the 10 h modulation albeit not as well pronounced as for Pioneer 10 or Ulysses. A comparison with the id4 and id5 counting rates shows a principle anticorrelation of counting rates and the spectral index. The result of an ordinal autocorrelation of the Pioneer 11 id5 channel is shown in Fig. 11. The principal 10 h rocking of the counting rates is well emphasised. However,

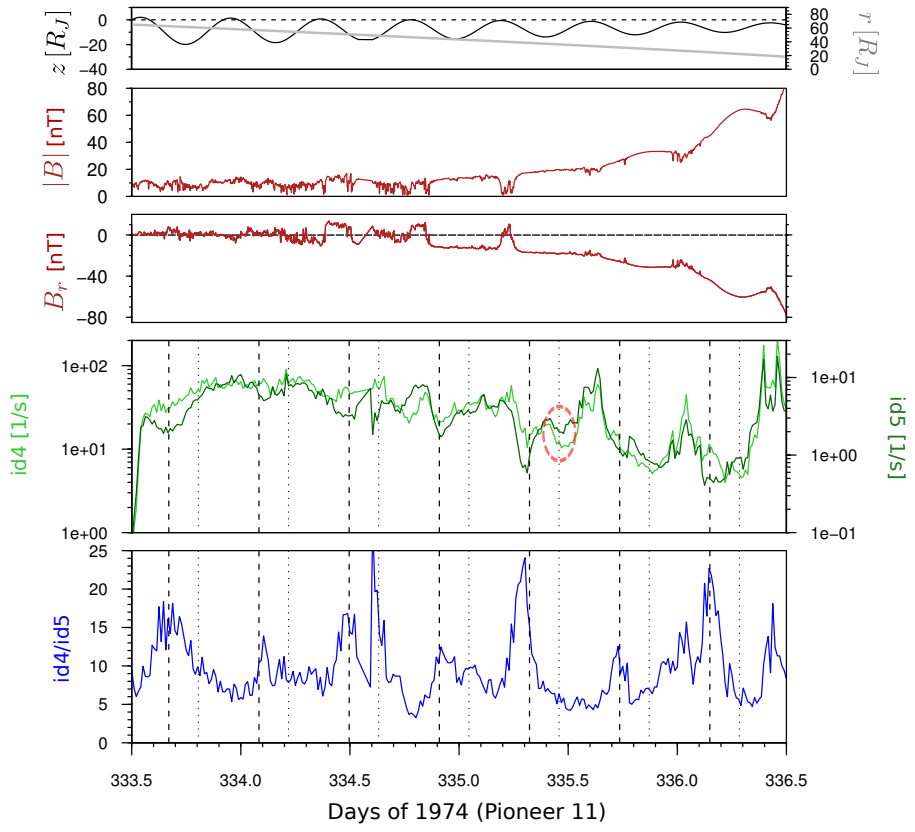

Fig. 10. Pioneer 11 data for the spacecraft's inbound pass from day 333.5 to 336.5 in 1974, showing the same quantities as Fig. 7. Compared to Pioneer 10 or Ulysses, the 10 h periodicity of the Jovian clock is weakly pronounced but visible. However, there is no evidence of a consistent pattern of minor peaks.

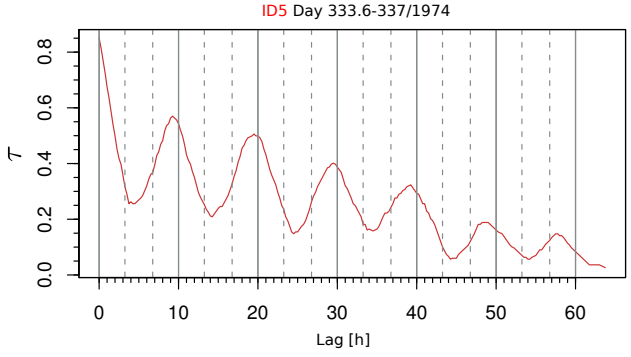

Fig. 11. Ordinal correlation analysis for the id5 energy channel of Pioneer 11. No evidence of minor peaks is present in the data.

no evidence of the presence of minor peaks in the spectral index or associated local counting rate minima can be identified. Note that we avoid showing a figure similar to Fig. 9 since no further conclusions can be drawn from it because of the lack of minor peaks.

5 Conclusions

In this work we presented an analysis and comparison of Ulysses and Pioneer 10/11 MeV electron data inside the Jovian magnetosphere during the spacecraft's flyby manoeuvres in February 1992 (Ulysses) and December 1973/1974 (Pioneers). We focused on the temporal variation in the counting rates and spectral index of the MeV electrons besides the well-known Jovian clock mechanism in the outer and middle regions of the Jovian magnetosphere at low magnetic latitudes. Another periodic modulation of about 10 h (minor peaks) could be identified in the Ulysses data (previously not discussed in detail in the literature) besides the spectral modulation generally attributed to the Jovian clock mechanism. This variation resembles the clock modulation: a steeper spectral index (approximated by the ratio of two adjacent energy channels) is associated with a decrease of the counting rates and vice versa. However, these increases and decreases have much smaller amplitudes than the ones related to the clock variation. Indeed, the minor peaks of the spectral index are associated with local minima in the counting rates while general maxima of MeV electron increase, forming a double-peak structure. The minor peaks appear

to trail the phase of the clock mechanism (major peaks) by ~ 3.25 h. The minor peaks are observed when the spacecraft is located at low magnetic latitudes, implying a connection with the magnetospheric current sheet. A comparison with the times of observation of the minor peaks and actual current sheet crossings in the middle magnetosphere showed an asymmetric behaviour in the sense that the minor peaks were observed when Ulysses crossed the current sheet from south to north. This implies an azimuthal asymmetry of the spectral index of MeV electrons along the current sheet.

A comparison with Pioneer data partly confirmed the existence of the minor peaks. However, while the Pioneer 10 MeV electron data show the double-peaked structure in the outer magnetosphere associated with minor peaks in the electron spectrum, there is no evidence of any proper modulation besides the clock mechanism in the Pioneer 11 data. The events found in the Pioneer 10 data show a phase shift with respect to the major peaks of ~ 3.25 h (i.e. a similar value as for the Ulysses events).

In the following we compare the occurrence of minor peaks observed by Ulysses with the spacecraft's distance from a rigid current sheet and the current sheet model developed by Khurana and Schwarzl (2005). The distance of a rigid current sheet from Jupiter's equator is calculated by

$$z_{\text{rigid}} = \rho \tan\theta_{\text{d}} \cos(\lambda - \lambda_0), \tag{1}$$

where ρ is the cylindrical distance of the spacecraft from the planet, $\theta_{\text{d}} = 9.6°$ the tilt angle of the dipole, and λ the longitude (System III). The prime meridian (i.e. the northernmost extent of the current sheet) is given as $\lambda_0 = 20.4°$.

A more realistic current sheet model was proposed by Khurana and Schwarzl (2005). This model takes into account an alignment of the current sheet with the solar wind flow direction at large distances as well as a bend-back of magnetic field lines and finite information propagation times. In this model, the distance of the magnetosphere from the equator is given by

$$z_{cs} = \left(\sqrt{(x_{\text{h}} \tanh(x/x_{\text{h}}))^2 + y^2}\right) \tan\theta_{\text{d}} \cos(\phi - \phi_0) + x(1 - \tanh(|x_{\text{h}}/x|) \tan\theta_{\text{s}}. \tag{2}$$

Here, x_{h} is the hinging distance, and x and y the spacecraft's position in the Jupiter–Sun–orbital coordinate system. The angle between the Jupiter–Sun vector and Jupiter rotational equator defines θ_{s} and is $\approx -1.1°$ during Ulysses' flyby in February 1992. Note that $\phi = 360° - \lambda$ in Eq. (2).

The distance of the spacecraft from the current sheet can then be calculated by $\Delta z = z_{s/c} - z_{cs}$. Figure 12 shows this distance as a function of time for the rigid disc (top), the Khurana model using their best fit value for the hinging distance (i.e. $x_{\text{h}} = 47\ R_{\text{J}}$). The bottom panel shows the same model but for a hinging distance that is much larger than the distance of the magnetopause (r_{mp}) from the planet: the hinging of the current sheet is neglected. The blue dots correspond to

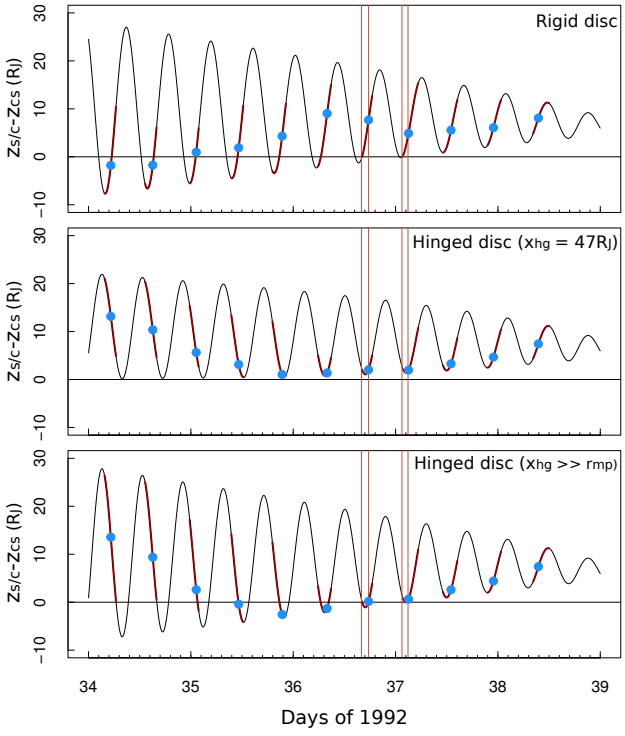

Fig. 12. The distance of Ulysses from the nominal current sheet (in units of Jovian radii) as a function of time for three different current models is shown. The top panel assumes a rigid current sheet, the middle panel a current sheet as described by the model of Khurana and Schwarzl (2005) using a standard hinging distance of $x_{\text{h}} = 47\ R_{\text{J}}$. The bottom panel is the Khurana model using a neglectable hinging of the current sheet (i.e. a hinging distance being much larger than the sunward extension of the magnetopause (r_{mp})).

times where the maximum of the minor peaks is observed; the red segments define the time intervals between the two minima bounding the minor peak. The four red vertical lines indicate the two pairs of observed current sheet crossings.

The simple rigid current sheet model does not match the actually observed current sheet crossings: the calculated current sheet crossings occur too early. The hinged current sheet models describe the observed times of current sheet crossings much better. However, using the best fit value for the hinged distance, $x_{\text{h}} = 47\ R_{\text{J}}$ (Khurana and Schwarzl, 2005), the excursion of the current sheet with respect to the spacecraft does not fit the data. Assuming an almost infinite hinging distance (bottom panel) gives the best fit to the observed current sheet crossings.

Comparing the occurrence of the minor peaks with respect to the distance of the spacecraft from the current sheet, these events generally seem to occur at low magnetic latitudes but do not exactly coincide with the current sheet. In particular, the model of Khurana and Schwarzl (2005) after day ~ 36.0 when Ulysses was located in the middle magnetosphere gives

a better agreement between low magnetic latitudes and the occurrence of minor peak.

Although the minor peaks cannot be exactly related to current sheet crossings, we conclude that the newly discovered minor peaks are a strong hint for an influence of the current sheet onto the temporal evolution of the spectral index. Thus, a model explaining this behaviour should include not only temporal effects (as in the clock model) but also spatial effects as suggested by disc and anomaly models.

Acknowledgements. The Ulysses project is supported under grant No. 50 OC 0105 by the German Bundesministerium für Wirtschaft through the Deutsches Zentrum für Luft- und Raumfahrt (DLR). This work has been also supported by the Deutsche Forschungsgemeinschaft under grant No. HE-3279/10-1. The partial financial support of the South African National Research Foundation (NRF) is acknowledged. We also acknowledge the National Space Science Data Center and R. B. McKibben, Principal Investigator of the COSPIN/HET instrument, and A. Balogh, Principal Investigator of the VHM/FMG instrument, for providing data via the Ulysses data system.

Topical Editor L. Blomberg thanks two anonymous referees for their help in evaluating this paper.

References

Anagnostopoulos, G. C., Marhavilas, P. K., Sarris, E. T., Karanikola, I., and Balogh, A.: Energetic ion populations and periodicities near Jupiter, J. Geophys. Res., 103, 20055–20074, 1998.

Balogh, A., Beek, T. J., Forsyth, R. J., Hedgecock, P. C., Marquedant, R. J., Smith, E. J., Southwood, D. J., and Tsurutani, B. T.: The magnetic field investigation on the ULYSSES mission – Instrumentation and preliminary scientific results, Astron. Astrophys. Sup. Ser., 92, 221–236, 1992.

Bandt, C.: Ordinal time series analysis, Ecological modelling, 182, 229–238, 2005.

Chenette, D. L., Conlon, T. F., and Simpson, J. A.: Bursts of relativistic electrons from Jupiter observed in interplanetary space with the time variation of the planetary rotation period, J. Geophys. Res., 79, 3551, doi:10.1029/JA079i025p03551, 1974.

Dessler, A. J. and Hill, T. W.: High-order magnetic multipoles as a source of gross asymmetry in the distant Jovian magnetosphere, J. Geophys. Res., 2, 567–570, 1975.

Fillius, W. and Knickerbocker, P.: The phase of the ten-hour modulation in the Jovian magnetosphere (Pioneers 10 and 11), J. Geophys. Res., 84, 5763–5772, 1979.

Hess, S. L. G., Bonfond, B., Zarka, P., and Grodent, D.: Model of the Jovian magnetic field topology constrained by the Io auroral emissions, J. Geophys. Res., 116, A05217, doi:10.1029/2010JA016262, 2011.

Hoogeveen, G. W., Phillip, J. L., and Dougherty, M. K.: Ulysses observations of corotation lags in the dayside Jovian magnetosphere: An evaluation of the hinged magnetosdisc and magnetic anomaly models, J. Geophys. Res, 101, 21439–21446, 1996.

Joy, S. P., Kivelson, M. G., Walker, R. J., Khurana, K. K., Russell, C. T., and Ogino, T.: Probabilistic models of the Jovian magnetopause and bow shock locations, J. Geophys. Res., 107, 1309, doi:10.1029/2001JA009146, 2002.

Khurana, K. K. and Schwarzl, H. K.: Global structure of Jupiter's magnetospheric current sheet, J. Geophys. Res., 110, A07227, 2005.

Krupp, N., Keppler, E., Korth, A., Fränz, M., Balogh, A., and Dougherty, M. K.: Three-dimensional particle anisotropies in and near the plasma sheet of Jupiter observed by the EPAC instrument onboard the Ulysses spacecraft, Planet. Space Sci., 41, 953–966, 1993.

Lentz, G. A., McKibben, R. B., O'Gallagher, J. J., Perkins, M., Simpson, J. A., and Tuzzolino, A. J.: Heliospheric Intensity Gradients of Galactic Cosmic Ray Nuclei and Electrons From Pioneer 10, International Cosmic Ray Conference, 2, 743–748, 1973.

Press, W. H., Teukolsky, S. A., Vetterling, W. T., and Flannery, B. P.: Numerical recipes in FORTRAN. The art of scientific computing, Cambridge: University Press, 2nd Edn., 1992.

Simpson, J. A., Anglin, J. D., Balogh, A., Bercovitch, M., Bouman, J. M., Budzinski, E. E., Burrows, J. R., Carvell, R., Connell, J. J., Ducros, R., Ferrando, P., Firth, J., Garcia-Munoz, M., Henrion, J., Hynds, R. J., Iwers, B., Jacquet, R., Kunow, H., Lentz, G., Marsden, R. G., Mckibben, R. B., Müller-Mellin, R., Page, D. E., Perkins, M., Raviart, A., Sanderson, T. R., Sierks, H., Treguer, L., Tuzzolino, A. J., Wenzel, K. P., and Wibberenz, G., The ULYSSES Cosmic Ray and Solar Particle Investigation, Astron. Astrophys. Sup. Ser., 92, 365–399, 1992a.

Simpson, J. A., Anglin, J. D., Balogh, A., Burrows, J. R., Cowley, S. W. H., Ferrando, P., Heber, B., Hynds, R. J., Kunow, H., and Marsden, R. G.: Energetic charged-particle phenomena in the Jovian magnetosphere – First results from the ULYSSES COSPIN collaboration, Science, 257, 1543–1550, 1992b.

van Allen, J. A., Baker, D. N., Randall, B. A., and Sentman, D. D.: The magnetosphere of Jupiter as observed with Pioneer 10. 1. Instrument and principal findings, J. Geophys. Res., 79, 3559–3577, 1974.

Vasyliunas, V. M. and Dessler, A. J.: The magnetic-anomaly model of the Jovian magnetosphere – A post-Voyager assessment, J. Geophys. Res., 86, 8435–8446, 1981.

Waldrop, L. S., Fritz, T. A., Kivelson, M. G., Khurana, K., Krupp, N., and Lagg, A.: Jovian plasma sheet morphology: particle and field observations by the Galileo spacecraft, Planet. Space Sci., 53, 681–692, 2005.